

# Image Deblurring in Super-resolution Framework

Srimanta Mandal

School of Computing and Electrical Engineering  
Indian Institute of Technology Mandi, India  
Email: in.srimanta.mandal@ieee.org

Anil Kumar Sao

School of Computing and Electrical Engineering  
Indian Institute of Technology Mandi, India  
Email: anil@iitmandi.ac.in

**Abstract**—In all image processing applications, it is important to extract the appropriate information from an image. But often the captured image is not clear enough to give the required information due to the imaging environment. Thus, it is essential to enhance the clarity of the image by some post-processing techniques. Image deblurring is one of such techniques to remove the blurry effect of the captured image. This paper looks into this problem in a different way, where the deblurring of an image is addressed by solving image super-resolution problem. The blurred image is first down-sampled and then it is fed to the super-resolution framework to produce the deblurred high resolution image. In addition, the proposed approach states the requirement of edge preservation in the problem. The experimental results are comparable with the existing image deblurring algorithms.

## I. INTRODUCTION

Several image processing applications like medical imaging, surveillance etc. need good quality of image for appropriate information extraction. But often this purpose can't be achieved due to the limitations of the imaging ambience (lens focus, size of imaging sensor, image capturing environment etc.). As a result the captured image is sometimes blurry, which is a problem and can be described mathematically as

$$\mathbf{y} = \mathbf{H}\mathbf{x} + \mathbf{z}, \quad (1)$$

where the blurred image  $\mathbf{y} \in \mathbb{R}^a$  is captured during imaging with approximated blur operator  $\mathbf{H} \in \mathbb{R}^{a \times a}$  and noise  $\mathbf{z} \in \mathbb{R}^a$ . Image deblurring seeks to recover the original scene  $\mathbf{x} \in \mathbb{R}^a$  from the blurry-noisy image  $\mathbf{y}$ . In other words  $\mathbf{x}$  needs to be deconvoluted from the blur kernel  $\mathbf{H}$  to remove the blur, as blurry image is assumed to be produced by convolving the blur kernel with the original scene. Thus the image deblurring problem is also known as blur deconvolution and is addressed in different ways in the literature. All these works can be broadly classified into two categories: i) blind deconvolution of blur kernel [1], [2] and ii) non-blind deconvolution of blur kernel [3], [4]. The approaches belong to the first class doesn't require any prior knowledge about the blur type, which is related to the real scenario. But the performance of these approaches mostly depend on the estimation of blur parameter from the given image which is difficult to estimate. Thus, when the blur type is given a priori due to known imaging environment, the second type of deconvolution is useful and proposed approach belongs to this category.

In this paper, the deblurring/blur deconvolution problem is addressed by solving image super-resolution (SR) problem, where a down-sampled low resolution (LR) image is super-resolved to a high resolution (HR) image. The motivation behind the different perspective of viewing the deblurring

problem can be justified using the super-resolution framework (see Fig. 1), where sub-pixel shifted LR images are fed to the SR system to produce a HR image [5]. If we look into the SR system, we can observe that the third block is deblurring and noise-removal, which is our main task here. So, multiple LR images produced from multiple blurred images can act as input to the SR system. But multiple blurred images of the target scene are difficult to obtain, such that the generated LR images are related to each other by sub-pixel precision. This issue can be addressed by some SR approaches, where a single LR image is required as input [6]–[9] to produce the required HR image. Thus, if the down-sampled version of the blurred image can be fed to the single image SR system, the deblurring problem can be solved.

Image super-resolution is an ill-posed problem, as many HR images can produce the same LR image. Thus some regularization techniques are required to make the problem well-posed. Several regularization techniques are available in the literature [10]–[12]. In current scenario, sparse domain regularization is producing better results due to its efficient capability of signal representation under certain condition. We have used the sparse domain representation to solve the stated problem. In addition, an edge preserving constraint is added to the problem as edge information is perceptually significant [9]. Experimental results show that the proposed SR framework for solving deblurring problem is comparable with the existing deblurring approaches.

The rest of the paper is organized as follows: Section II explains the sparse domain framework required for solving the deblurring problem. Section III maps the deblurring problem as SR problem. The experimental results are given in section IV and the paper is concluded in section V.

## II. IMAGE DEBLURRING USING SPARSE DOMAIN REPRESENTATION

In sparse domain representation, a signal  $\mathbf{x}$  can be represented as a linear combination of few columns of a dictionary matrix  $\mathbf{A} \in \mathbb{R}^{a \times \alpha}$  ( $\alpha > a$ ) with the help of a vector  $\mathbf{c} \in \mathbb{R}^\alpha$ , whose most of the elements are zero or close to zero [13]. Mathematically it can be written as:

$$\mathbf{x} = \mathbf{A}\mathbf{c}. \quad (2)$$

Thus the deblurring model as stated in (1) become

$$\mathbf{y} = \mathbf{H}\mathbf{A}\mathbf{c} + \mathbf{z}, \quad (3)$$

and can be solved with sparsity constraint as

$$\hat{\mathbf{c}} = \arg \min_{\mathbf{c}} \|\mathbf{c}\|_0 \text{ s.t. } \|\mathbf{y} - \mathbf{H}\mathbf{A}\mathbf{c}\|_2^2 \leq \epsilon, \quad (4)$$

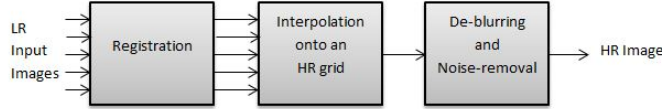


Fig. 1. Super-resolution framework

where  $\|\cdot\|_0$  gives the number of non-zero elements of a vector and  $\epsilon$  is a small value, defines the error threshold of restoration. But evaluating equation (4) requires combinatorial search, which is NP-hard and  $l_1$ -norm is the closest convex approximation of the  $l_0$ -norm [14]. Thus with a Lagrangian multiplier  $\lambda$ , the above constrained optimization problem can be written in an unconstrained closed form as

$$\hat{\mathbf{c}} = \arg \min_{\mathbf{c}} \{ \|\mathbf{y} - \mathbf{HAc}\|_2^2 + \lambda \|\mathbf{c}\|_1 \}. \quad (5)$$

Solving equation (5) requires a suitable choice of dictionary  $\mathbf{A}$  for efficient sparse representation of signal. The dictionary can be derived analytically or by learning from example images [15]. Analytical dictionary has the advantage of fast implementation but it may not be suitable to represent the complex structure of natural image appropriately [15]. Therefore, learning based dictionaries are preferred over the analytical dictionaries despite of their higher computational complexity. It has been shown that dictionaries, learned for local image structures can represent the image better than a single over-complete dictionary [8]. Thus multiple sub-dictionaries can be learned from the training images instead of a single over-complete dictionary. In this paper multiple sub-dictionary learning is opted as mentioned in reference [8], where the sub-dictionaries are derived by selecting the principal components from some similar patches, clustered by K-means clustering. During restoration those dictionaries are selected adaptively.

### III. PROPOSED APPROACH OF DEBLURRING USING SR FRAMEWORK

Let's analyze the blur model in mathematical point of view by multiplying  $\mathbf{D}$  to both side of equation (1)

$$\mathbf{Dy} = \mathbf{DHx} + \mathbf{Dz}, \quad (6)$$

which can be written as

$$\mathbf{y}_1 = \mathbf{DHx} + \mathbf{z}_1, \quad (7)$$

where  $\mathbf{y}_1 \in \mathbb{R}^b$  and  $\mathbf{z}_1 \in \mathbb{R}^b$  ( $b < a$ ) are the down-sampled version of  $\mathbf{y}$  and  $\mathbf{z}$  respectively. The equation (7) explains that the  $\mathbf{y}_1$  is produced after down-sampling (using operator  $\mathbf{D} \in \mathbb{R}^{b \times a}$ ) the blurred and noisy image. In deblurring problem (1) the motive is to find  $\mathbf{x}$  from  $\mathbf{y}$ , but the equation (7) states to find out  $\mathbf{x}$  from  $\mathbf{y}_1$ , which is a SR problem. Thus if one can feed a down-sampled version of the blurry-noisy image to the SR system, it can produce the desired deblurred HR image. The proposed framework can be seen in Fig. 2.

Now, the cost function as stated in equation (5) can be modified as

$$\hat{\mathbf{c}} = \arg \min_{\mathbf{c}} \{ \|\mathbf{y}_1 - \mathbf{DHAc}\|_2^2 + \lambda \|\mathbf{c}\|_1 \}. \quad (8)$$

It has been found that edge plays an important role during SR [9]. Thus we have incorporated an edge preserving

constraint in equation (8), such that the edge of the deblurred image follow the LR image, generated from the input blurry image [9].

Here one may debate about adding the edge preserving constraint in the problem as in blurred image, every details of the image are smoothed out. It can be justified by comparing the intensity profile plots (Fig. 3) of the generated LR images from the input blurred image and the original image. One can observe that both profiles are similar at the point of strong edges, when the gradient of the intensity profile is very high.

We can also observe that intensity profile does not match in the range of 40-50 pixel along the horizontal scan line, which could be due to aliasing phenomenon. This observation reinforce the idea of using edge preserving constraint in the proposed approach. Thus the cost function stated in equation (8) can be modified as:

$$\hat{\mathbf{c}} = \arg \min_{\mathbf{c}} \{ \|\mathbf{y}_1 - \mathbf{DHAc}\|_2^2 + \lambda \|\mathbf{c}\|_1 \} \quad (9)$$

$$\text{s.t. } \|\mathbf{E}_g\{\mathbf{y}_1\} - \mathbf{E}_g\{\mathbf{DHAc}\}\|_2^2 \leq \epsilon,$$

where  $\mathbf{E}_g$  represents the edge magnitude gradient operator, which is applied to obtain the magnitude gradient  $\mathbf{e}_g = \sqrt{\mathbf{e}_0^2 + \mathbf{e}_{90}^2}$ .<sup>1</sup> The optimization problem (9) can be solved for  $\mathbf{c}$  using iterative thresholding algorithm [16]. Once  $\hat{\mathbf{c}}$  is obtained the deblurred image can be achieved by  $\hat{\mathbf{x}} = \mathbf{A}\hat{\mathbf{c}}$ .

### IV. EXPERIMENTAL RESULTS

In this paper Gaussian blur kernel of size  $15 \times 15$  with standard deviation 3 is used to generate the blurred image. In addition, white Gaussian noise with standard deviation  $\sqrt{2}$  and 2 are separately added in the blurred image to verify the robustness of the proposed approach. The blurred images of dimension  $256 \times 256$  are down-sampled by a factor 2 to generate LR image, which is fed to the SR system. The SR system will generate the deblurred-HR image with the help of a dictionary created by patch of size  $5 \times 5$  pixels. The performance of the proposed approach is compared against some existing image deblurring methods [3], [4], [17] in terms of peak signal to noise ratio (PSNR) and structural similarity index (SSIM) [18] in Table I & II<sup>2</sup> for different levels of noise. One can observe that the performance of the proposed method is relatively better than the existing approaches for most of the images.

We have also compared the deblurred image obtained using the proposed approach along with an existing work [4] for the *cameraman* and *pepper* in Fig. 4 & 5, respectively. It can be observed that, in smoother regions, the artifacts have come

<sup>1</sup>Here  $\mathbf{e}_0$  and  $\mathbf{e}_{90}$  represents the vertical edge evidence and horizontal edge evidence respectively [9].

<sup>2</sup>Bold fonts represent the best values (PSNR & SSIM) in that row.

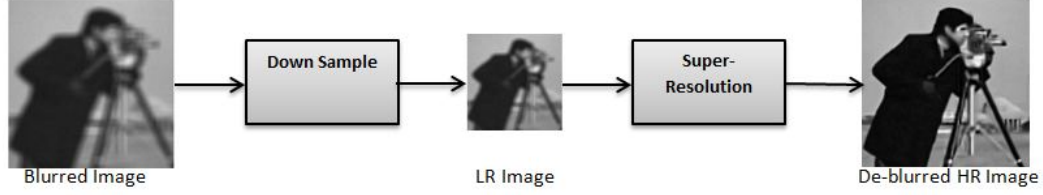


Fig. 2. Proposed framework for solving deblurring problem

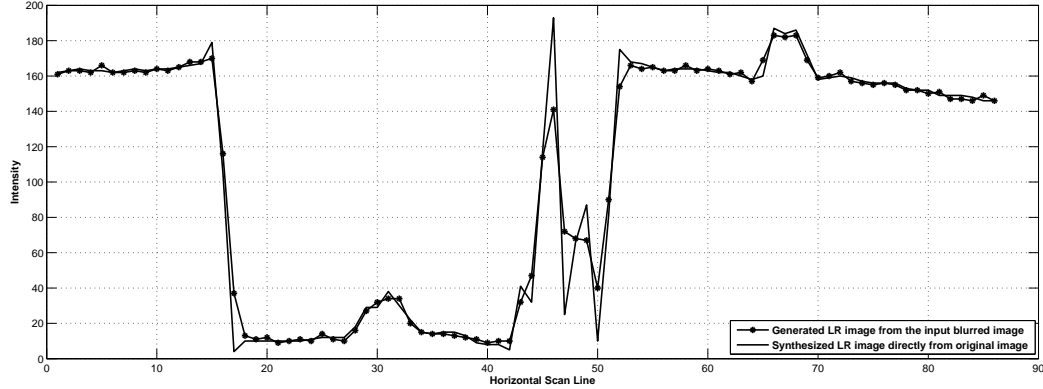


Fig. 3. Comparison of intensity profiles for the *cameraman* image. The original size of the input blurred *cameraman* is  $258 \times 258$  and the image is down-sampled by factor 3 to size  $86 \times 86$ .

TABLE I  
RESULTS OF IMAGE DEBLURRING FOR GAUSSIAN BLUR ( $\sigma = 3$ ) WITH NOISE LEVEL  
 $\sigma_n = \sqrt{2}$ .

Images	Variational Bayes [3]		Constrained TV [17]		Wavelet [4]		Proposed Approach	
	PSNR	SSIM	PSNR	SSIM	PSNR	SSIM	PSNR	SSIM
Baboon	19.85	0.3011	<b>20.01</b>	0.3396	19.49	0.3451	19.77	<b>0.3494</b>
Barbara	23.19	0.5892	23.22	0.5971	21.89	0.6035	<b>23.65</b>	<b>0.6393</b>
Bike	21.20	0.5515	21.90	0.6137	21.13	0.5781	<b>22.09</b>	<b>0.6273</b>
Boats	24.77	0.6688	25.53	0.7056	21.93	0.6571	<b>26.36</b>	<b>0.7476</b>
Cameraman	22.59	0.7187	23.26	<b>0.7483</b>	21.93	0.6801	<b>23.35</b>	0.7416
Hat	28.29	0.7924	<b>28.90</b>	<b>0.8100</b>	25.70	0.7429	28.73	0.8024
Parrot	25.21	0.7949	25.96	0.8080	23.69	0.7756	<b>26.76</b>	<b>0.8440</b>
Pentagon	22.09	0.4387	22.48	0.4881	22.22	0.5163	<b>22.90</b>	<b>0.5400</b>
Peppers	24.94	0.7236	<b>25.58</b>	0.7411	22.75	0.7165	25.35	<b>0.7722</b>
Straw	19.33	0.2749	19.76	0.3502	19.87	0.3711	<b>20.03</b>	<b>0.3878</b>
<b>Average</b>	23.15	0.5854	23.66	0.6202	22.06	0.5986	<b>23.90</b>	<b>0.6452</b>

TABLE II  
RESULTS OF IMAGE DEBLURRING FOR GAUSSIAN BLUR ( $\sigma = 3$ ) WITH NOISE LEVEL  
 $\sigma_n = 2$ .

Images	Variational Bayes [3]		Constrained TV [17]		Wavelet [4]		Proposed Approach	
	PSNR	SSIM	PSNR	SSIM	PSNR	SSIM	PSNR	SSIM
Baboon	19.79	0.2905	<b>20.00</b>	<b>0.3389</b>	19.48	0.3439	19.58	0.3357
Barbara	23.07	0.5776	23.19	0.5933	21.88	0.6010	<b>23.53</b>	<b>0.6289</b>
Bike	20.97	0.5324	21.88	0.6125	21.13	0.5776	<b>21.96</b>	<b>0.6137</b>
Boats	24.63	0.6602	25.48	0.7032	21.91	0.6542	<b>25.88</b>	<b>0.7316</b>
Cameraman	22.36	0.7130	<b>23.23</b>	<b>0.7465</b>	21.91	0.6749	22.77	0.7347
Hat	28.27	0.7913	<b>28.86</b>	<b>0.8084</b>	25.68	0.7409	28.57	0.7980
Parrot	25.05	0.7907	25.92	0.8053	23.68	0.7739	<b>26.29</b>	<b>0.8351</b>
Pentagon	21.89	0.4200	22.46	0.4876	22.20	0.5152	<b>22.65</b>	<b>0.5202</b>
Peppers	24.38	0.7034	<b>25.50</b>	0.7373	22.73	0.7133	25.39	<b>0.7667</b>
Straw	19.24	0.2590	19.75	0.3499	<b>19.86</b>	<b>0.3708</b>	19.73	0.3612
<b>Average</b>	22.96	0.5738	23.63	0.6183	22.05	0.5966	<b>23.64</b>	<b>0.6326</b>

down in the proposed approach. In addition the edges of the images are sharpened in the deblurred image derived using the proposed approach (see marked regions in Fig. 4 & 5). This emphasizes the requirement of edge preservation in the proposed framework.

One assumption of the proposed approach is that the chosen down-sampling factor should not be very high to avoid the aliasing effect. In this work we have chosen 2 as down-sampling factor to produce the best result.

## V. CONCLUSION

This paper proposed a new direction to look at the image deblurring problem in the framework of image SR. The

blurred-noisy image is down-sampled to prepare the input data to the SR system. The output of the SR system produces deblurred-HR image using the constraint of edge consistency with the input LR image. The experimental results shows the comparability of the proposed approach with some of the existing approaches. In future, we would like to combine the deblurred images derived in the proposed framework using different down-sampling factor.

## REFERENCES

- [1] E. Faramarzi, D. Rajan, and M. Christensen, "Unified blind method for multi-image super-resolution and single/multi-image blur deconvolution," *IEEE Transactions on Image Processing*, vol. 22, no. 6, pp. 2101–2114, 2013.



Fig. 4. Results of deblurring for the image *Cameraman* with noise level  $\sigma_n = \sqrt{2}$ : Left-to-right–a) Original image, b) Blurred-noisy image, c) Restored by the approach [4] and d) Restored by the proposed approach.

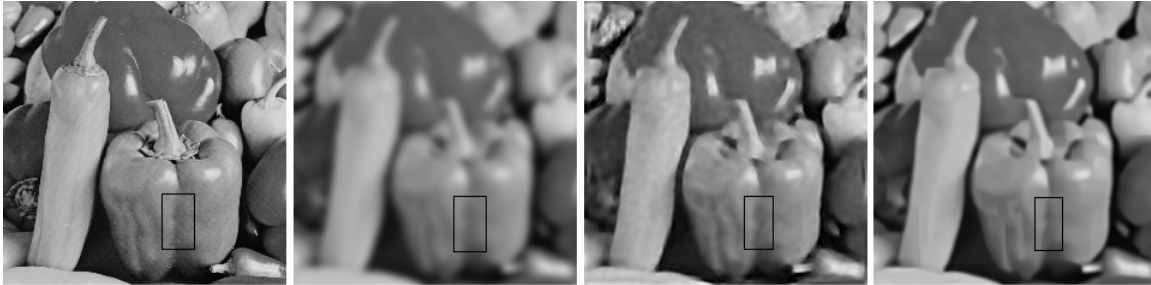


Fig. 5. Results of deblurring for the image *Peppers* with noise level  $\sigma_n = 2$ : Left-to-right–a) Original image, b) Blurred-noisy image, c) Restored by the approach [4] and d) Restored by the proposed approach.

- [2] T. Chan and C.-K. Wong, "Total variation blind deconvolution," *IEEE Transactions on Image Processing*, vol. 7, no. 3, pp. 370–375, 1998.
- [3] G. Chantas, N. Galatsanos, R. Molina, and A. Katsaggelos, "Variational bayesian image restoration with a product of spatially weighted total variation image priors," *IEEE Transactions on Image Processing*, vol. 19, no. 2, pp. 351–362, 2010.
- [4] M. Figueiredo and R. Nowak, "A bound optimization approach to wavelet based image deconvolution," in *IEEE International Conference on Image Processing - ICIP 2005, Genoa, Italy*, September 2005, pp. 782–785.
- [5] S. C. Park, M. K. Park, and M. G. Kang, "Super-resolution image reconstruction: a technical overview," *IEEE, Signal Processing Magazine*, vol. 20, no. 3, pp. 21 – 36, may 2003.
- [6] J. Yang, J. Wright, T. Huang, and Y. Ma, "Image super-resolution via sparse representation," *IEEE Transactions on Image Processing*, vol. 19, no. 11, pp. 2861–2873, Nov. 2010.
- [7] R. Zeyde, M. Elad, and M. Protter, "On single image scale-up using sparse-representations," in *Curves and Surfaces*. Springer, 2012, vol. 6920, pp. 711–730.
- [8] W. Dong, L. Zhang, G. Shi, and X. Wu, "Image deblurring and super-resolution by adaptive sparse domain selection and adaptive regularization," *IEEE Transactions on Image Processing*, vol. 20, no. 7, pp. 1838 –1857, july 2011.
- [9] S. Mandal and A. K. Sao, "Edge preserving single image super resolution in sparse environment," in *IEEE International Conference on Image Processing (ICIP)*, 2013.
- [10] N. Galatsanos and A. Katsaggelos, "Methods for choosing the regularization parameter and estimating the noise variance in image restoration and their relation," *IEEE Transactions on Image Processing*, vol. 1, no. 3, pp. 322 –336, jul 1992.
- [11] L. I. Rudin, S. Osher, and E. Fatemi, "Nonlinear total variation based noise removal algorithms," *Physica D: Nonlinear Phenomena*, vol. 60, no. 14, pp. 259 – 268, 1992.
- [12] J. Bioucas-Dias, "Bayesian wavelet-based image deconvolution: a GEM algorithm exploiting a class of heavy-tailed priors," *IEEE Transactions on Image Processing*, vol. 15, no. 4, pp. 937 –951, april 2006.
- [13] M. Elad, *Sparse and Redundant Representations - From Theory to Applications in Signal and Image Processing*. Springer, 2010.
- [14] D. L. Donoho, "For most large underdetermined systems of equations, the minimal  $l_1$ -norm near-solution approximates the sparsest near-solution," *Communications on Pure and Applied Mathematics*, vol. 59, no. 7, pp. 907–934, 2006.
- [15] R. Rubinstein, A. Bruckstein, and M. Elad, "Dictionaries for sparse representation modeling," *Proceedings of the IEEE*, vol. 98, no. 6, pp. 1045 –1057, june 2010.
- [16] I. Daubechies, M. Defrise, and C. De Mol, "An iterative thresholding algorithm for linear inverse problems with a sparsity constraint," *Communications on Pure and Applied Mathematics*, vol. 57, no. 11, pp. 1413–1457, 2004.
- [17] A. Beck and M. Teboulle, "Fast gradient-based algorithms for constrained total variation image denoising and deblurring problems," *IEEE Transactions on Image Processing*, vol. 18, no. 11, pp. 2419–2434, 2009.
- [18] A. Hore and D. Ziou, "Image quality metrics: PSNR vs. SSIM," in *20th International Conference on Pattern Recognition (ICPR)*, aug. 2010, pp. 2366 –2369.